Electronic Supplementary Material (ESI) for Journal of Materials Chemistry A.
This journal is © The Royal Society of Chemistry 2018

Supplementary Information

PVP-capped CdS Nanopopcorns with Type-II Homojunctions for Highly Efficient Visible-Light-Driven Organic Pollutant Degradation and Hydrogen Evolution

Na Zhao,[a] Jing Peng,[a] Gang Liu,*[b] Youwei Zhang,[c] Wanying Lei,[b] Zhibin Yin,[a] Jiuqiang Li,[a] Maolin Zhai,*[a]

[a]College of Chemistry and Molecular Engineering, Radiochemistry and Radiation Chemistry KeyLaboratory of Fundamental Science, Beijing National Laboratory for Molecular Sciences, Peking University, Beijing 100871, P.R. China. *E-mail: mlzhai@pku.edu.cn

[b] CAS Key Laboratory of Standardization and Measurement for Nanotechnology, CAS Center for Excellence in Nanoscience, National Center for Nanoscience and Technology, Beijing 100190, P.R. China. E-mail: liug@nanoctr.cn

[c]Aviation Key Laboratory of Science and Technology on Stealth Materials, Beijing Institute of Aeronautical Materials, Beijing 100095, P. R. China

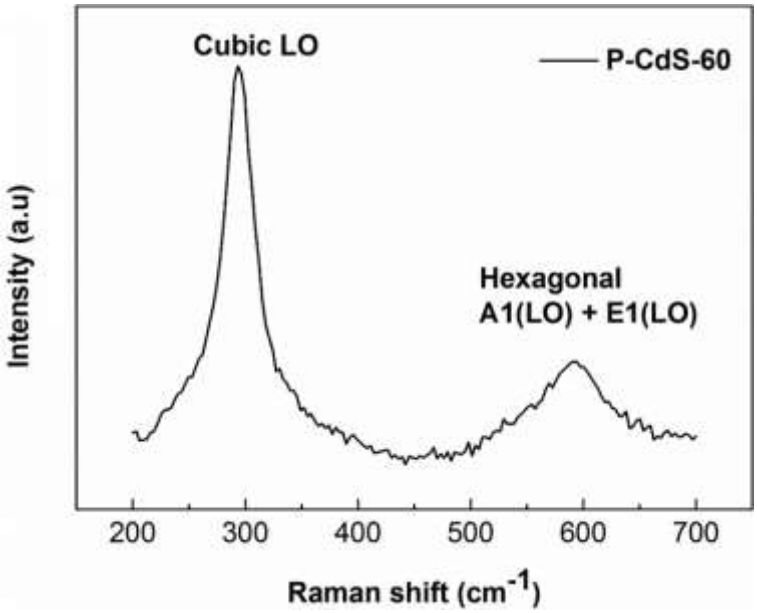

Fig. S1. Raman spectrum of P-CdS-60.

In Fig. S1, the first Raman scattering at ~293 cm^{-1} and the second scattering at ~591 cm^{-1} result from the cubic LO phonon and the hexagonal A_1(LO) + E_1(LO) phonons and their overtones, respectively[1, 2].

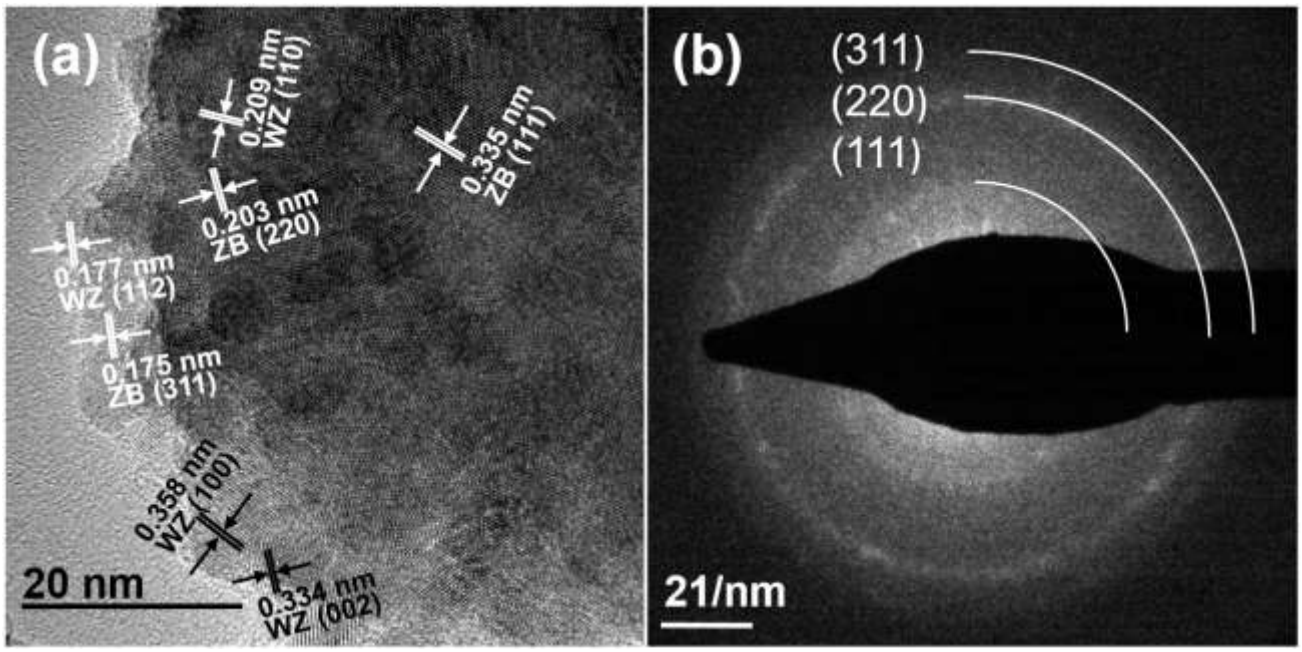

Fig. S2. (a) Typical HRTEM image of P-CdS-60. (b) Corresponding SAED patterns showing the randomly oriented polycrystallites with ZB phase as a predominant phase.

Typical HRTEM image of P-CdS-60 (Fig. S2a) exhibits lattice fringes with d spacings of 0.358, 0.334, 0.209, 0.177 nm, which is ascribed to the respective (100), (002), (110), (112) planes of WZ phase. And the lattice fringes with d spacings of 0.335, 0.203, 0.175 nm are in agreement with the (111), (220), and (311) planes of ZB phase, respectively.

The corresponding SAED pattern (Fig. S2b) displays that the P-CdS-60 consists of the randomly oriented polycrystallites. Three major broadening peaks labeled as (111), (220) and (311) can be assigned as the ZB phase, suggesting that the ZB phase is the major one.

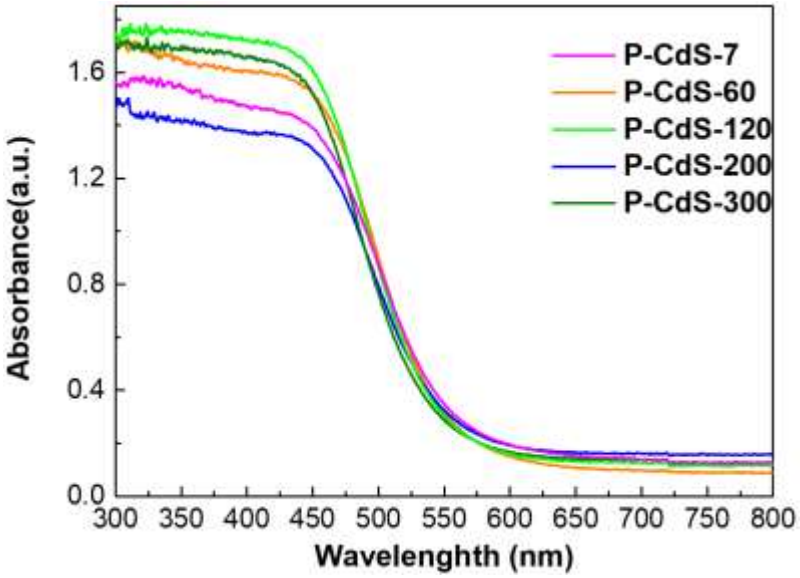

Fig.S3. DRUV-vis spectra for the PVP-capped CdS nanopopcorns grown at different dose rates, with a total absorbed dose of 300 kGy.

When the dose rate is decreased, the optical absorption edge of the CdS nanopopcorns is red-shifted to the longer wavelength.

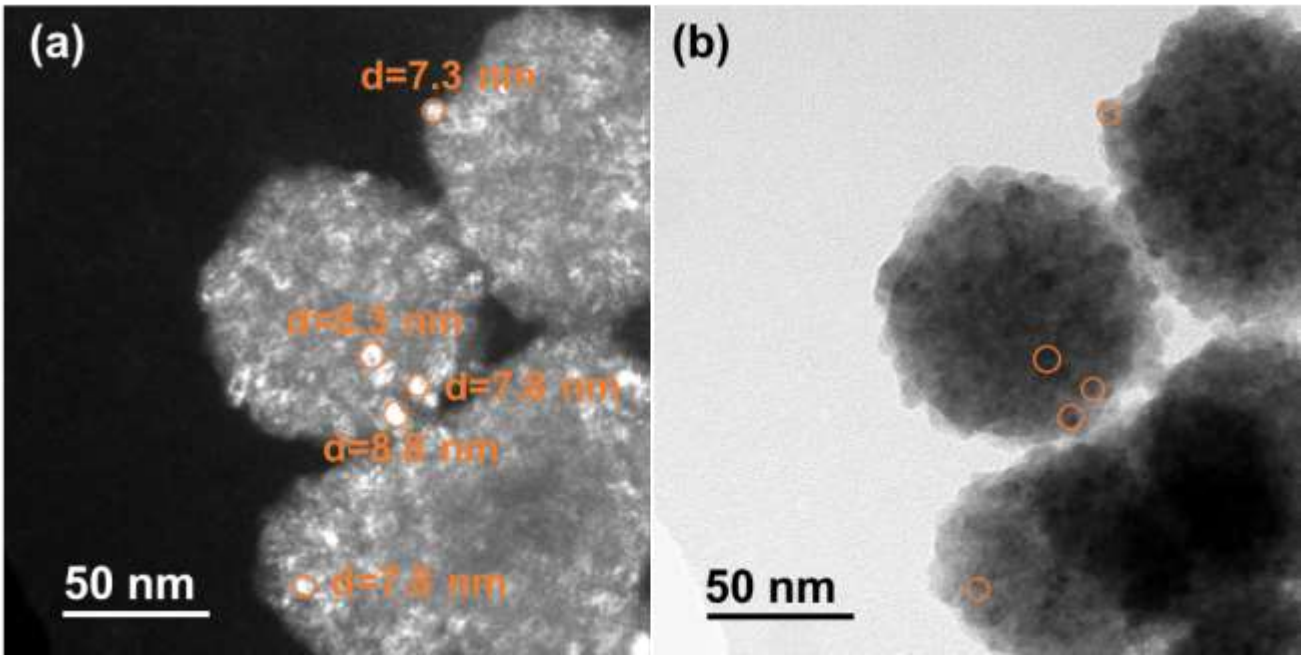

Fig. S4. (a) The dark field TEM image of P-CdS-7, (b) The corresponding bright field TEM image of P-CdS-7. The grain size is about 8 nm.

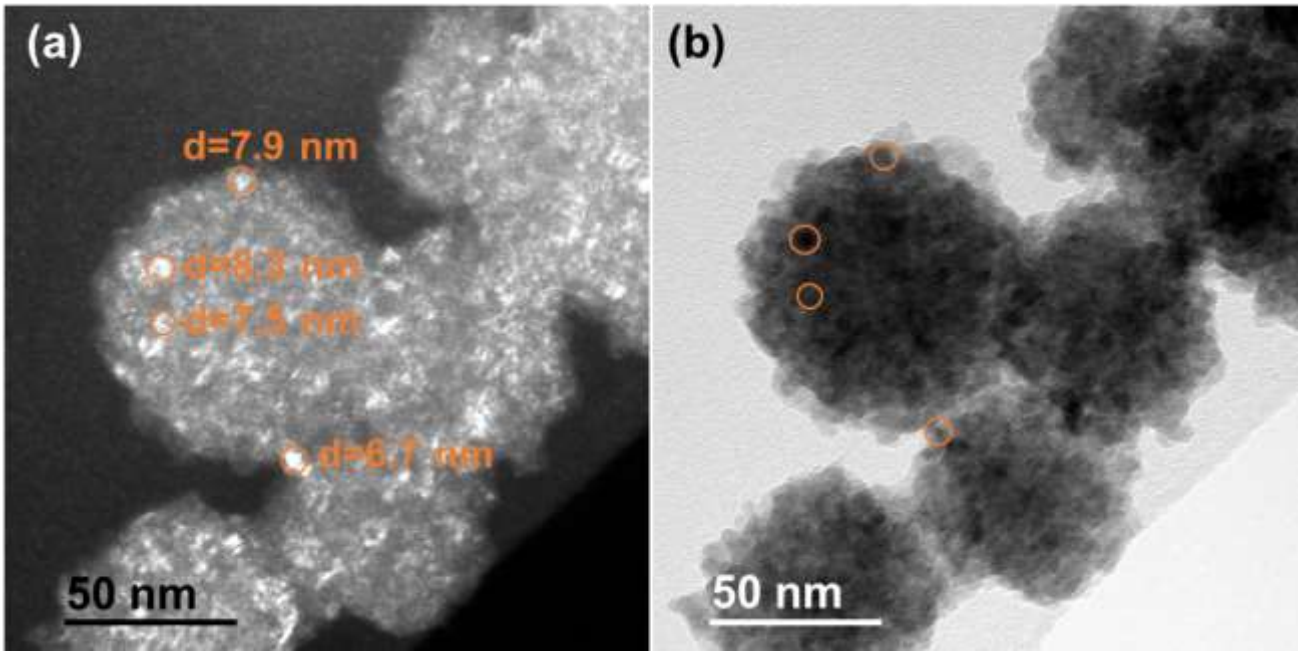

Fig. S5. (a) The dark field TEM image of P-CdS-60, (b) The corresponding bright field TEM image of P-CdS-60. The grain size is about 8 nm.

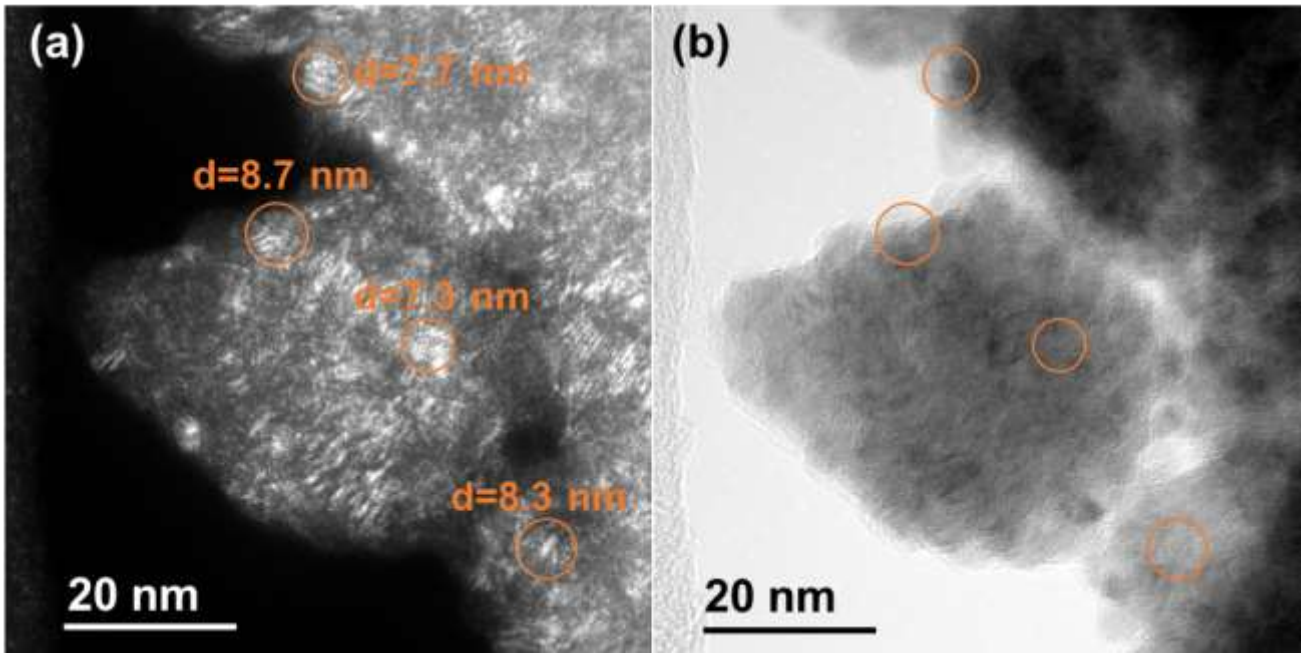

Fig. S6. (a) The dark field TEM image of P-CdS-120, (b) The corresponding bright field TEM image of P-CdS-120. The grain size is about 8 nm.

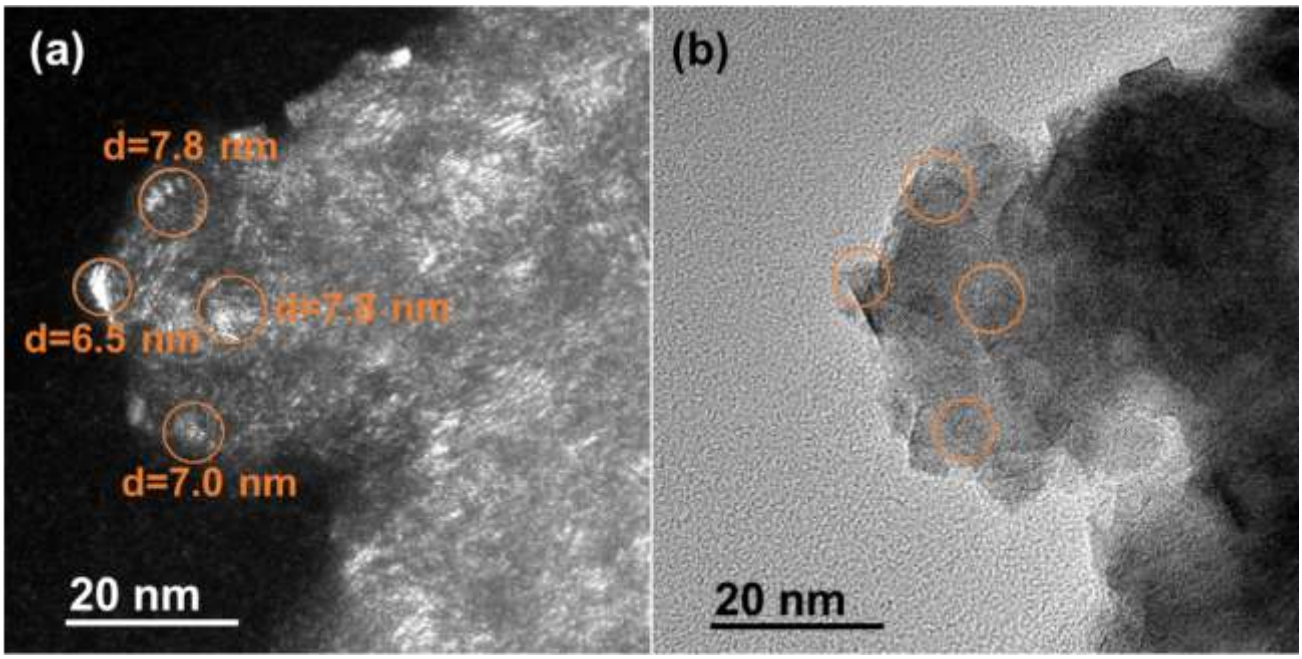

Fig. S7. (a) The dark field TEM image of P-CdS-200, (b) The corresponding bright field TEM image of P-CdS-200. The grain size is about 8 nm.

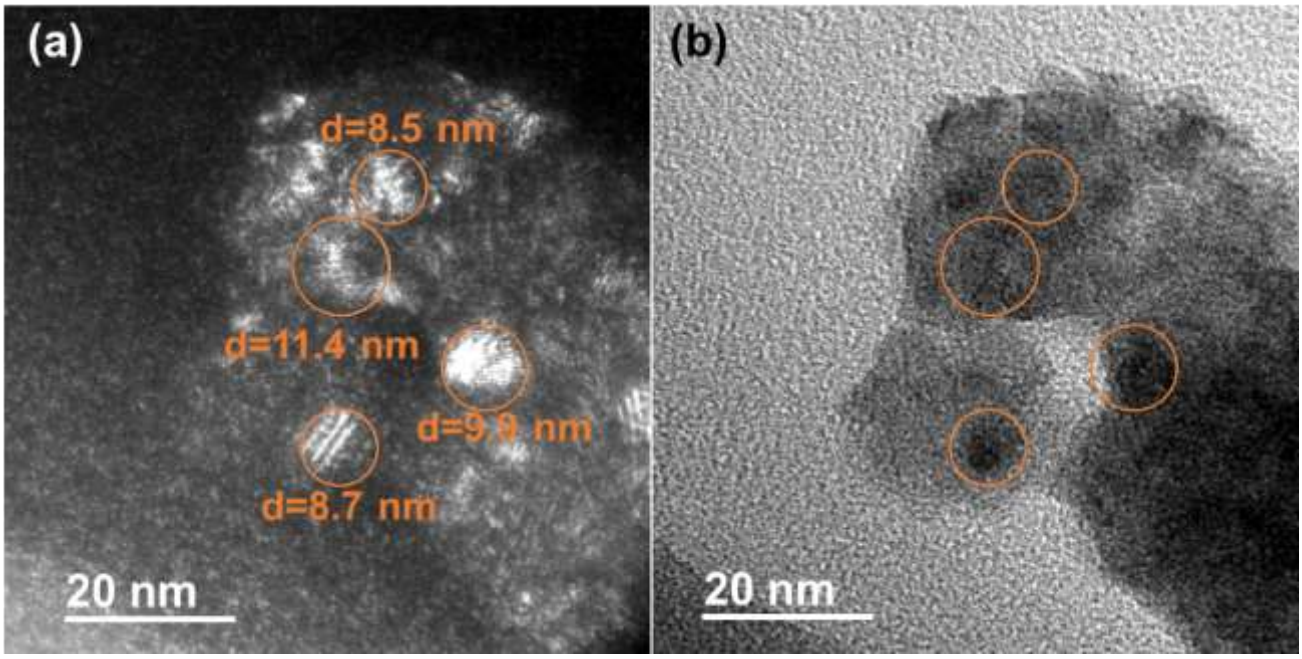

Fig. S8. (a) The dark field TEM image of P-CdS-300, (b) The corresponding bright field TEM image of P-CdS-300. The grain size is about 8 nm.

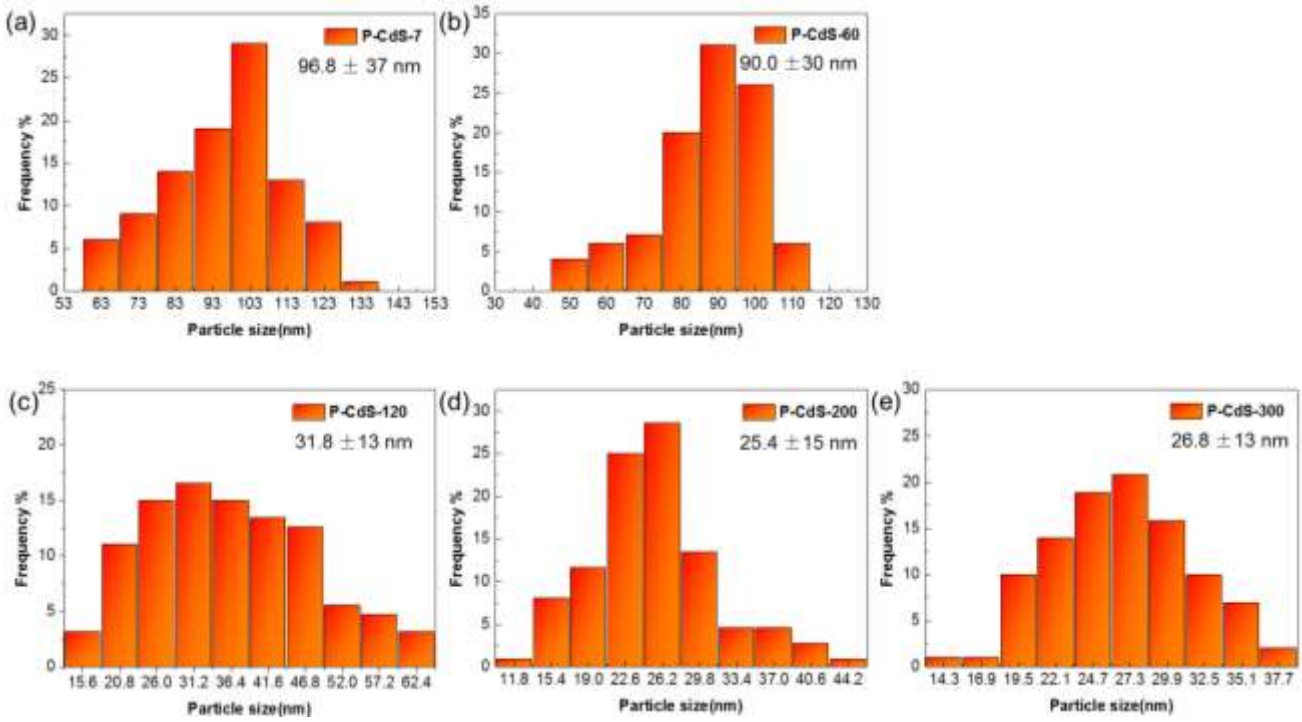

Fig. S9. The size distributions of PVP-capped CdS nanopopcorns grown at different dose rates: (a) 7, (b) 60, (c) 120, (d) 200 and (e) 300 Gy/min, which are obtained by the statistical analysis of 100 particles in Fig. 2a-e, respectively.

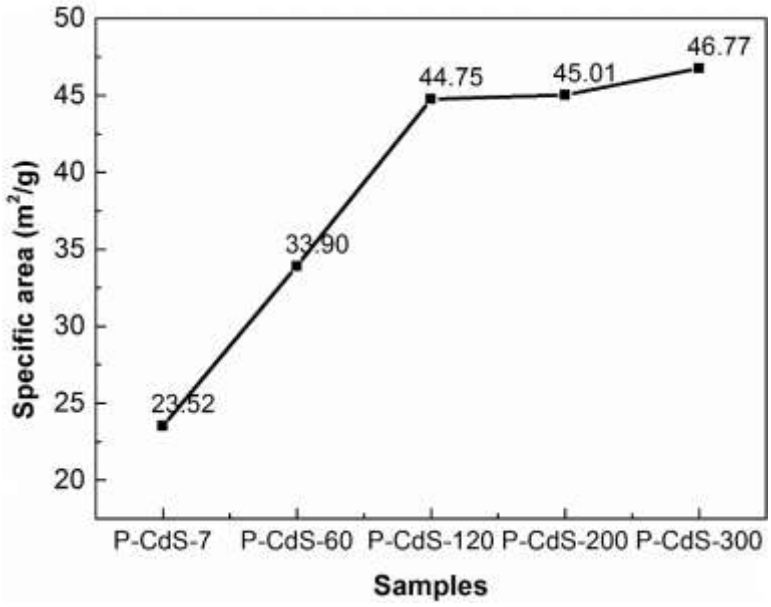

Fig. S10. The BET specific area of the PVP-capped CdS nanoparticles grown at different dose rates. The total dose is 300 kGy.

The BET specific area of the CdS nanoparticles increases from 23.52 to 46.77 m^2/g with increasing dose rate, which mainly results from the dose rate-dependent particle size.

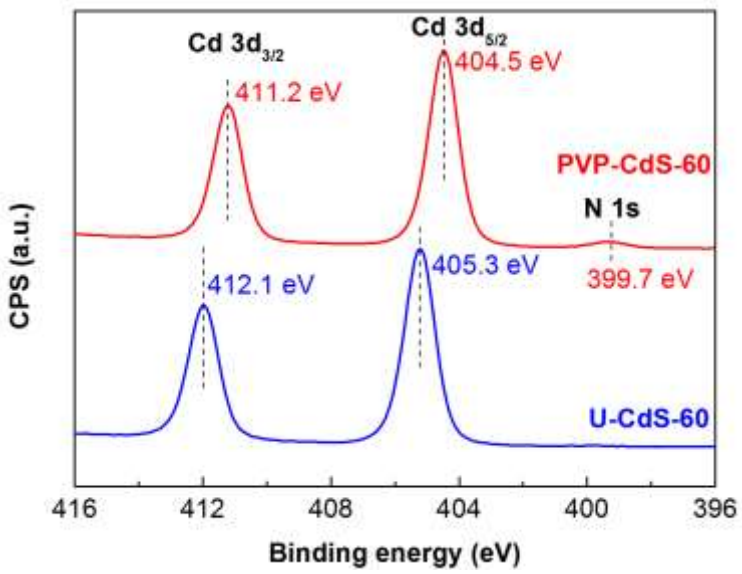

Fig. S11. The Cd 3d high-resolution XPS spectra of P-CdS-60 nanopopcorns and U-CdS-60 particles.

Cd $3d_{5/2}$ of PVP-CdS-60 is located at 404.50 eV, a negative shift (ca. 0.8 eV) with respect to that of U-CdS-60. The shift of Cd $3d_{5/2}$ to lower binding energies in P-CdS-60 is ascribed to the direct bonding between the C=O group of PVP with CdS[3].

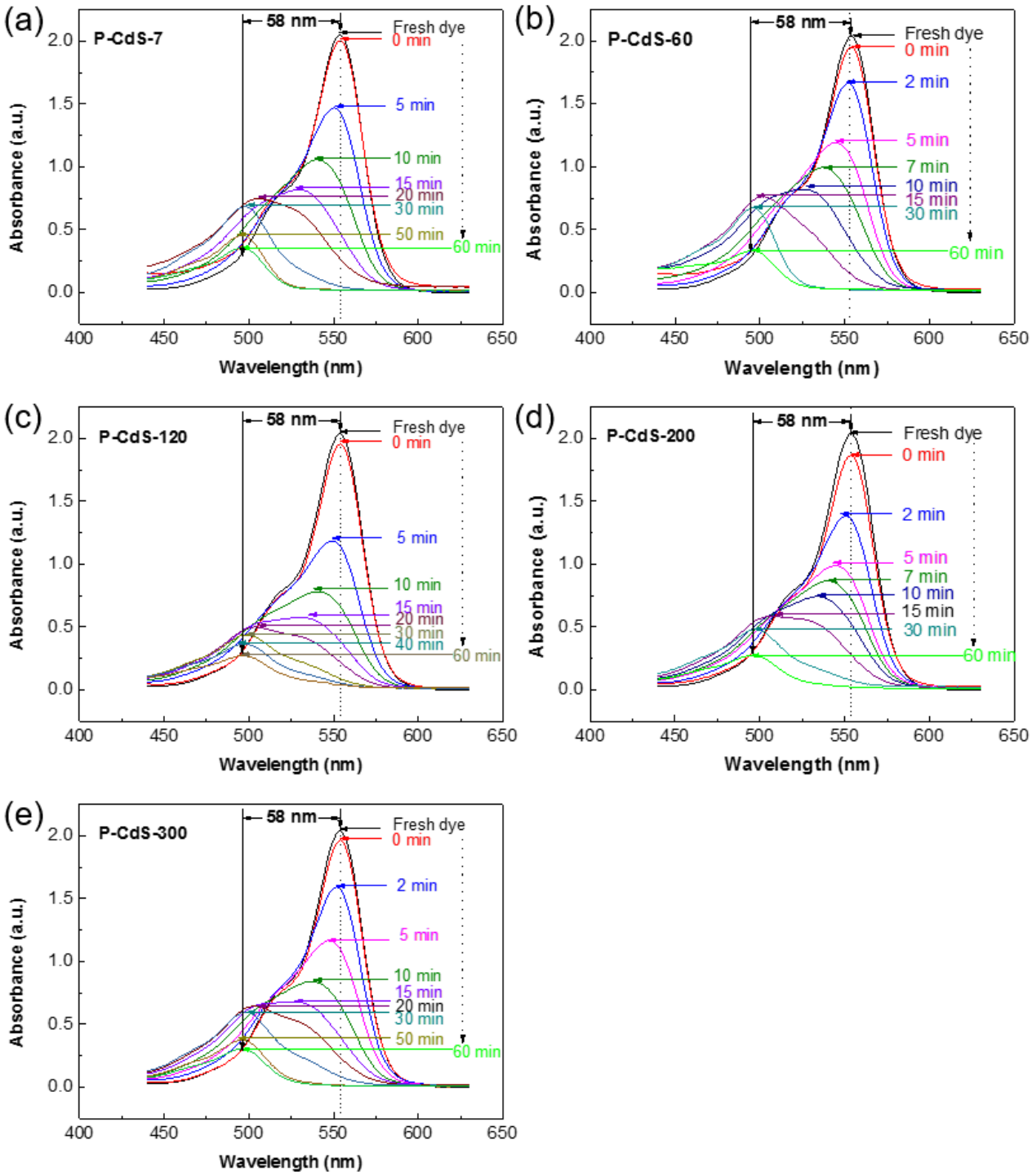

Fig. S12. Absorbance spectra of RhB photodegradation catalyzed by (a) P-CdS-7, (b) P-CdS-60, (c) P-CdS-120, (d) P-CdS-200, (e) P-CdS-300.

The absorption maximum of RhB at 553 nm is blue-shifted to 498 nm owing to the deethylation of the N,N,N',N'-tetra ethylated RhB molecule in a stepwise manner. Ethyl groups will be removed one by one, leading to its major absorption band shifted towards the blue regime, i.e., RhB (λ_{max}=553 nm), N,N,N'-tri-ethylated rhodamine(539 nm), N,N'-di-ethylated rhodamine (522 nm), N-ethylated

rhodamine (510 nm), and rhodamine (498 nm)[4, 5]. Fig. S13b-d illustrates when the photocatalysts are synthesized at lower dose rates, the rate of the deethylation pathways is relatively higher. For example, for P-CdS-60 synthesized at a relatively lower dose rate, upon visible-light illumination for 30 min the absorption band of RhB at 553 nm disappears completely while the absorption band at 498 nm appears. In contrast, for P-CdS-200 synthesized at a relatively higher dose rate, there are absorption bands at 553 nm, 539 nm, 522 nm, 510 nm, 498 nm upon visible-light illumination for 30 min, suggesting that the above five major RhB degradation-derived products still exist.

Calculations of the TON and TOF

The turnover number (TON) and turnover frequency (TOF) were calculated by using the following equations:

For RhB degradation:

$$TON = \frac{\text{moles of the degaradation for RhB}}{\text{moles of CdS}}$$

$$TOF = \frac{TON}{\text{reaction time (hours)}}$$

For hydrogen evolution:

$$TON = \frac{\text{moles of evolved } H_2}{\text{moles of CdS}}$$

$$TOF = \frac{TON}{\text{reaction time (hours)}}$$

Table S1. Comparison of TON and TOF for the photocatalytic RhB degradation by a series of CdS-based photocatalysts under visible-light illumination.

Sample	Amount of catalyst (mg)	Time (min)	Percentage (%)	TON	TOF (h^{-1})
P-CdS-7	20	20	87.34	1.31	3.94
P-CdS-60	20	20	98.65	1.48	4.45
P-CdS-120	20	20	89.57	1.35	4.04
P-CdS-200	20	20	91.79	1.38	4.14
P-CdS-300	20	20	88.69	1.33	4.00
U-CdS-60	20	20	49.91	0.75	2.25

Table S2. Comparison of TON and TOF for the hydrogen evolution by a series of CdS-based photocatalysts under visible-light illumination.

Sample	Amount of catalyst (mg)	Time (h)	Amount of H_2 evolution (μmol)	TON	TOF (h^{-1})
P-CdS-7	50	4	581.41	1.67	0.33
P-CdS-60	50	4	788.26	2.27	0.45
P-CdS-120	50	4	469.48	1.35	0.27
P-CdS-200	50	4	479.12	1.38	0.28
P-CdS-300	50	4	419.80	1.21	0.24

Table S3. Comparison of photocatalytic RhB degradation activity of representative CdS-based photocatalysts.

Photocatayst	crystalline phase	Light source	Amount of catalyst (mg)	Reaction solution	Time (min)	Percentage (%)	Activity (min^{-1})	Ref. (year)
CdS nanobubbles	ZB phase	300 W Xe arc lamp	0.15	RhB (24 ppm, 1.5 mL)	NA	NA	0.081	[6](2014)
CdS nanoparticles	WZ phase	500 W Xe lamp (λ> 420 nm)	3.5	RhB (5 ppm, 20ml)	35	28	NA	[7](2014)
CdS nanoparticles	WZ phase	halogen lamp (λ> 420 nm)	5	MB (24 ppm, 20 mL)	120	70	0.043	[8](2014)
CdS nanodots	ZB phase	500 W Xe lamp (λ> 400 nm)	100	RhB (10 ppm, 100 mL)	90	50	NA	[9](2016)
CdS dendrites	WZ phase	800 W Xe lamp	50	RhB (10 ppm, 200 mL)	220	98	NA	[10](2016)
CdS flowers	ZB and WZ phase	500 W Xe lamp	30	RhB (5 ppm, 40 mL)	150	85	NA	[11](2016)
CdS nanopaticles	WZ phase	300 W Xe lamp (λ> 420 nm)	100	RhB (5 ppm, 100 mL)	60	49	0.0111	[12](2016)
CdS nanoparticles	ZB and WZ phase	300 W Xe lamp (λ> 420 nm)	40	RhB (40 ppm, 100 mL)	120	20.5	0.0019	[13](2017)
PVP-capped CdS nanopopcoins	ZB-WZ homojunction	300 W Xe lamp (λ> 420 nm)	20	RhB (10 ppm, 100 mL)	15	95.5	0.211	this work

Table S4. Comparison of photocatalytic H_2 production rate of representative CdS-based photocatalysts.

Photocatayst	Crystalline phase	Co-catalyst	Light source	Reaction solution	Amount of H_2 evolution (μmol/g/h)	Ref. (year)
CdS nanopaticles	WZ phase	Pt (1 wt.%)	300 W Xe lamp (λ> 420 nm, 168 mW/cm^2)	Lactic acid	200	[14](2016)
CdS nanorods	WZ phase	a-MWCNTs (10 wt%) /MoS_2 (1 wt%)	300 W Xe lamp (λ> 400 nm)	Lactic acid	676	[15](2016)
CdS nanopaticles	WZ phase	WS_2 (40 wt%)	300 W Xe-lamp (λ> 420 nm)	Lactic acid	373.41	[16](2016)
CdS nanorods	WZ phase	Pt (0.2 wt.%)	300 W Xe lamp (λ> 400 nm)	Lactic acid	2540	[17](2017)
CdS nanopaticles	WZ phase	Pt (2 wt.%)	300 W Xe lamp (λ> 420 nm, 52.2 mW/cm^2)	Na_2SO_3+Na_2S	1259	[18](2017)
WZ@ZB CdS nanorods	ZB-WZ homojunction	No	300 W Xe lamp (λ> 420 nm, ~200 mW/cm^2)	Na_2SO_3+Na_2S	742.5	[19](2016)
CdS nanorods	ZB-WZ homojunction	No	300 W Xe-lamp (λ> 420 nm)	Na_2SO_3+Na_2S	1340	[20](2016)
PVP-capped CdS nanopopcoins	ZB-WZ homojunction	Pt (0.65 wt.%)	300 W Xe lamp (λ> 420 nm, 100 mW)	Lactic acid	3520	this work

References

1. O. ZelayaAngel, F. D. CastilloAlvarado, J. AvendanoLopez, A. EscamillaEsquivel, G. ContrerasPuente, R. LozadaMorales and G. TorresDelgado, *Solid State Commun.*, 1997, **104**, 161-166.
2. R. Rossetti, S. Nakahara and L. E. Brus, *J. Chem. Phys.*, 1983, **79**, 1086-1088.
3. A. M. Abdelghany, E. M. Abdelrazek and D. S. Rashad, *Spectroc. Acta Pt. A-Molec. Biomolec. Spectr.*, 2014, **130**, 302-308.
4. T. Watanabe, T. Takizawa and K. Honda, *J. Phys. Chem.*, 1977, **81**, 1845-1851.
5. W. J. Li, D. Z. Li, S. G. Meng, W. Chen, X. Z. Fu and Y. Shao, *Environ. Sci. Technol.*, 2011, **45**, 2987-2993.
6. Y. Kim, H. B. Kim and D. J. Jang, *J. Mater. Chem. A*, 2014, **2**, 5791-5799.
7. S. L. Wang, J. J. Li, X. D. Zhou, C. C. Zheng, J. Q. Ning, Y. J. Zhong and Y. Hu, *J. Mater. Chem. A*, 2014, **2**, 19815-19821.
8. N. Kumar, V. K. Komarala and V. Dutta, *Chem. Eng. J.*, 2014, **236**, 66-74.
9. Q. J. Fan, Y. N. Huang, C. Zhang, J. J. Liu, L. Y. Piao, Y. C. Yu, S. L. Zuo and B. S. Li, *Catal. Today*, 2016, **264**, 250-256.
10. Z. Yu, F. Y. Qu and X. Wu, *Dalton Trans.*, 2014, **43**, 4847-4853.
11. W. Z. Wang, Y. J. Lu, Y. F. Xu, K. L. Wu, J. R. Huang, C. C. Ji and S. O. Ryu, *Crystengcomm*, 2016, **18**, 4681-4687.
12. F. X. Wang, L. Liang, K. L. Chen and J. M. Sun, *J. Mol. Catal. A-Chem.*, 2016, **425**, 76-85.
13. H. B. Huang, Y. Wang, F. Y. Cai, W. B. Jiao, N. Zhang, C. Liu, H. L. Cao and J. Lu, *Front. Chem.*, 2017, **5**.
14. J. Z. Chen, X. J. Wu, L. S. Yin, B. Li, X. Hong, Z. X. Fan, B. Chen, C. Xue and H. Zhang, *Angew. Chem.-Int. Edit.*, 2015, **54**, 1210-1214.
15. F. Q. Zhou, J. C. Fan, Q. J. Xu and Y. L. Min, *Appl. Catal. B-Environ.*, 2017, **201**, 77-83.
16. X. Jia, M. Tahir, L. Pan, Z. F. Huang, X. W. Zhang, L. Wang and J. J. Zou, *Appl. Catal. B-Environ.*, 2016, **198**, 154-161.
17. X. L. Fu, L. Zhang, L. H. Liu, H. Li, S. G. Meng, X. J. Ye and S. F. Chen, *J. Mater. Chem. A*, 2017, **5**, 15287-15293.
18. M. C. Liu, D. W. Jing, Z. H. Zhou and L. J. Guo, *Nat. Commun.*, 2013, **4**.
19. K. Li, M. Han, R. Chen, S. L. Li, S. L. Xie, C. Y. Mao, X. H. Bu, X. L. Cao, L. Z. Dong, P. Y. Feng and Y. Q. Lan, *Adv. Mater.*, 2016, **28**, 8906-8911.
20. M. C. Liu, B. Wang, Y. Q. Zheng, F. Xue, Y. B. Chen and L. J. Guo, *Catal. Sci. Technol.*, 2016, **6**, 3371-3377.